

Cherenkov and Scintillation Light Separation in Organic Liquid Scintillators

J. Caravaca,^{1,2} F.B. Descamps,^{1,2} B.J. Land,^{1,2} M. Yeh,³ and G.D. Orebi Gann^{1,2}

¹*University of California, Berkeley, CA 94720-7300, USA*

²*Lawrence Berkeley National Laboratory, CA 94720-8153, USA*

³*Brookhaven National Laboratory, Upton, NY 11973-500, USA*

The CHErenkov / Scintillation Separation experiment (CHESS) has been used to demonstrate the separation of Cherenkov and scintillation light in both linear alkylbenzene (LAB) and LAB with 2g/L of PPO as a fluor (LAB/PPO). This is the first such demonstration for the more challenging LAB/PPO cocktail and improves on previous results for LAB. A time resolution of 338 ± 12 ps FWHM results in an efficiency for identifying Cherenkov photons in LAB/PPO of $70 \pm 3\%$ and $63 \pm 8\%$ for time- and charge-based separation, respectively, with scintillation contamination of $36 \pm 5\%$ and $38 \pm 4\%$. LAB/PPO data is consistent with a rise time of 0.75 ± 0.25 ns.

The ability to separate Cherenkov and scintillation light in liquid scintillator (LS) detectors would enable a new generation of optical detectors that could achieve directional reconstruction at low energy thresholds, with powerful particle identification and event discrimination capabilities [1]. Such a detector would have applications across particle, nuclear, and astrophysics including a next-generation search for neutrinoless double beta decay, unprecedented sensitivity to solar neutrinos, proton decay, and sensitivity to the neutrino mass hierarchy and CP violation if deployed in a neutrino beam [1, 2].

Cherenkov light is emitted at the picosecond scale after ionization, while typical time constants of organic liquid scintillators are at the nanosecond level; signal separation via photon arrival time is thus a theoretical possibility. Separation by charge is feasible if an excess of Cherenkov photons can be observed above the isotropic scintillation background. A recent work [3] has demonstrated time separation in pure linear alkylbenzene (LAB). For experimental use LAB is most often deployed in combination with a fluor such as PPO to improve light yield by an order of magnitude. This substantially increases the physics reach of the experiment, but makes separation more challenging due to both significantly enhanced scintillation yield, which can swamp the Cherenkov component, and faster timing. Sub-ns time resolution becomes critical to achieve good separation.

This letter reports results from the CHErenkov Scintillation Separation experiment (CHESS) on Cherenkov / scintillation signal separation in pure LAB and LAB with 2 g/L of PPO (LAB/PPO). An overview of the apparatus is presented, along with calibrations relevant to LS data. Further details of CHESS are described in [4].

CHESS is designed to achieve sub-ns time resolution in photon detection using ultra-fast Hamamatsu H11934 photomultiplier tubes (PMTs) [5] with a transit time spread (TTS) of 300 ps FWHM, read out with a 5 GHz CAEN V1742 digitizer [6]. 12 PMTs are positioned in a cross shape below a cylindrical UV-transmitting acrylic (UVT) target vessel (Fig. 1). A UVT block optically coupled between target and PMTs acts as an optical

propagation medium. The primary source is through-going cosmic muons. Two muon tags placed above and below the setup provide a coincidence signal used to select muons within 6° from vertical, in order to produce a Cherenkov ring in a known location and scintillation light across the PMT array. A vertical hollow beneath the target prevents cosmic muons producing Cherenkov light in the propagation medium. The setup is surrounded by four Eljen [7] scintillator panels with 4π coverage of cosmic muons traversing the target. These are used to veto cosmic shower events, which do not produce a single clear Cherenkov ring. The majority of muon events are high energy and produce Cherenkov light at the maximum Cherenkov angle (48° in LAB; 41° in water). The spacing between target and PMTs is optimized to produce Cherenkov rings in the outer-most PMTs for LAB and LAB/PPO. The target height is optimized to ensure the width of the Cherenkov ring is approximately equal to the size of the PMT front face, to maximize photon detection efficiency. Isotropic scintillation light is detected across the entire PMT array. As a result, the inner PMTs are hit only by scintillation photons and the outer PMTs by Cherenkov and scintillation photons (Fig. 1).

In order to optimize the detector configuration and interpret results, a complete Monte Carlo (MC) simulation has been built using the RAT-PAC toolkit [8]. Geometry, material properties, PMT response, and DAQ effects are taken into account as described in [4]. A custom cosmic muon generator has been written following the Gaisser modified zenith and energy distribution [9]. Particle propagation and medium ionization is modeled by Geant4 [10], with the exception of optical photons, which are handled by the RAT-PAC custom absorption and re-emission model. The time profile of scintillation light is modeled according to the triple exponential decay described in [11], with the addition of a single exponential rise time. LS properties are taken from [3, 12–14].

Cosmic muon events are collected with water, LAB, and LAB/PPO targets by triggering acquisition when the lower muon tag crosses a pre-defined threshold, set well above the single photoelectron (SPE) level to avoid trig-

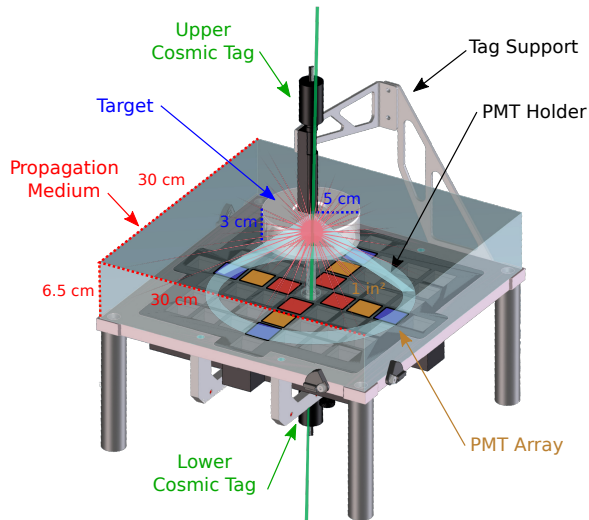


FIG. 1. CHESH schematic. The PMT array can hold up to 53 PMTs; the 12 slots occupied for this study are color coded by radius: red and orange for those hit primarily by scintillation photons, and blue for those that detect the Cherenkov ring.

gering on PMT dark noise. Coincidence with the upper tag is required offline. A coincidence rate of $\sim 4 \mu/\text{day}$ is expected. Four weeks of data is taken with each target.

The PMT response is characterized using calibration data prior to deployment of a LS target [4]. The PMT gain is measured using Cherenkov light from a ^{90}Sr beta source with a water target, in order to provide a population of SPE hits. SPE charge distributions are collected for each PMT and fit with a Gaussian. The mean of the Gaussian is taken as a measure of PMT gain, which is used to estimate the number of PE based on the charge of a hit PMT. PMT pulse shapes were collected for events close to the mean of the SPE distribution and an average was found across all PMTs. This was fit with a log normal distribution, which is used to model pulse shapes in the MC. Per-channel time delays due to electronic delays, cable delays, and the PMT transit time are measured using an LED, and cross-checked using Cherenkov light produced by cosmic muons passing through the propagation medium. Values are on the order of 100s of ps.

Event selection criteria have been defined in order to obtain a clean sample of single cosmic muon events passing vertically through the target. Optimization of the selection is performed using a water-filled target and Monte Carlo simulation. A loose charge cut above the noise peak for the upper and lower muon tags and the veto panel immediately beneath the setup ensures coincidence events. To remove cosmic shower events, a detected charge compatible with electronic noise is required in every scintillator panel other than the one immediately below the setup. Large pulses from the PMT

array induce crosstalk in the muon tag that occasionally trigger acquisition. This instrumental background can be identified by the characteristic oscillatory behavior of the resulting signals in the muon tags. The number of low frequency harmonic modes is calculated for the muon tag waveforms using a Fast Fourier Transform algorithm provided by ROOT [15]. Actual muon signals have a sizable low frequency component so events with a small low frequency component are removed. Another undesirable background is caused by muons clipping the propagation medium, or producing secondary particles that can themselves generate photons in that medium. Both create some Cherenkov light contamination across the PMT array, primarily on the innermost PMTs. These events have been modeled in simulation [4], and the expected number of PE from these events is seen to be appreciably greater even than the expected scintillation yield, due to the proximity of production in the propagation medium. Between 30 and 400 PE of Cherenkov photon contamination is expected on the inner PMTs for these events, whereas the expected scintillation yield on these PMTs is ~ 30 PEs for LAB and ~ 300 PEs for LAB/PPO. The summed charge on these PMTs can therefore be used to identify and remove these events. A threshold is applied to the total number of PEs across the 4 inner PMTs, $\text{NPE}_{\text{inner}}$, rejecting events that have $\text{NPE}_{\text{inner}} > 40$ for LAB and $\text{NPE}_{\text{inner}} > 500$ for LAB/PPO [4].

The signal from each PMT is digitized at 5 GHz and the resulting waveforms are analyzed to extract the hit time and charge. The hit time is calculated using a fixed threshold approach, with a channel-dependent threshold set at $1/4$ of the SPE peak. The charge is defined as the pedestal-corrected integral of the pulse in a 135 ns window, with the pedestal calculated on a per-waveform basis. Traces with a baseline fluctuation larger than 5 mV peak-to-valley in the pedestal region are not analyzed.

A simple algorithm reconstructs the event time as the median of the four most prompt hits. Hit-time residuals are calculated as the difference between the PMT hit time and the event time, corrected for photon time-of-flight and the measured per-channel time delays.

The time resolution of CHESH is determined from the hit-time residual distribution of Cherenkov events produced by cosmic muons with a water target [4]. The resolution is found to be 338 ± 12 ps FWHM.

A comparison of data to MC prediction for water show that the simulation slightly under-predicts the detector resolution, likely due to PMT-to-PMT variations in the PMT TTS and pulse shapes, or multi-photon effects. This is corrected for in simulations for all targets by including an additional smearing on the hit-time residual distributions of $\sigma = 214$ ps [4].

After applying event selection criteria, 117 ring candidates were identified in the LAB data set. An example event is shown in Fig. 2, while the average across the data set is shown in Fig. 3 for both time and charge. A clear

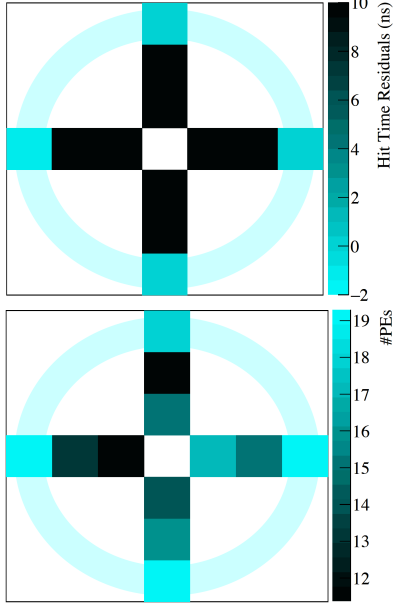


FIG. 2. A single ring candidate event in LAB. (Top) Hit-time residual and (Bottom) number of PE versus PMT position.

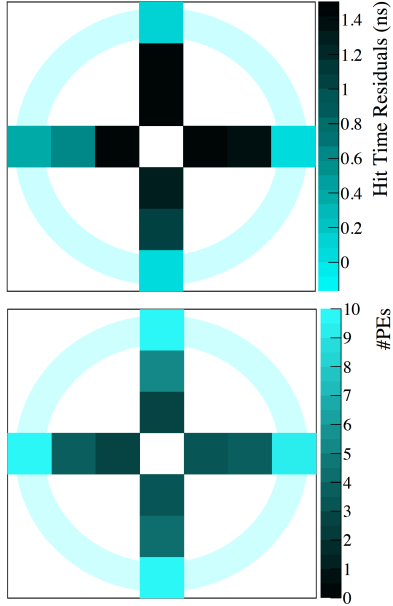


FIG. 3. (Top) Average hit-time residuals and (Bottom) average number of PE versus PMT position for ring candidate events in LAB.

ring structure can be observed in both cases.

The hit-time residual distributions for LAB are shown in Fig. 4 individually for the three radial PMT groupings, for data and MC. The outer PMTs, where the Cherenkov ring is expected, register the earliest hits, while the distributions for the middle and inner groups are broader and peak later, consistent with scintillation light. Early features in the inner and middle PMT groups are primar-

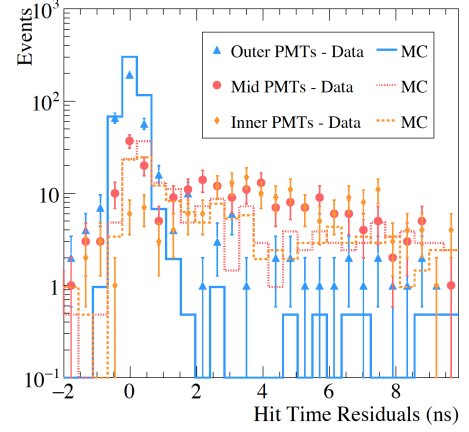


FIG. 4. Hit-time residual distributions in LAB for data and MC.

ily due to Cherenkov light contamination from secondary electrons. The MC reproduces data well, supporting the conclusion that true Cherenkov / scintillation separation has been observed. The first photon hits on the outer PMTs are due to fast Cherenkov photons, whereas middle and inner PMT hits are due to scintillation light. The ratio of hit counts between the two populations can thus be used to quantify the Cherenkov / scintillation separation. A time cut ($t < t_c$) is optimized in order to maximize separation. The efficiency of identifying Cherenkov hits is defined as the fraction of outer PMT hits that occur before t_c . The scintillation contamination is given by the fraction of hits occurring before t_c that are due to scintillation *i.e.* hits with $t < t_c$ on the inner and middle PMTs. The analysis is performed using both LED- and muon-extracted time delays and the difference taken as a systematic uncertainty. The optimal timing cut for LAB is $t_c = 0.4$ ns, yielding $83 \pm 2(\text{stat}) \pm 2(\text{syst})\%$ detection efficiency for Cherenkov hits, with contamination of $11 \pm 1(\text{stat}) \pm 0(\text{syst})\%$. Better separation might be achieved by eliminating the Cherenkov contamination in the inner and middle PMTs via improvements to the CHES apparatus.

Charge separation can be achieved by taking the ratio of charge in a prompt window to that in the full event window for each hit PMT and comparing this for the different populations of hits. The result for LAB is shown in Fig. 5. The separation is defined in an analogous manner to that for time: a threshold is optimized to maximize the Cherenkov hit detection efficiency and minimize scintillation contamination. A threshold of $Q_{\text{ratio}} = 0.09$ gives a Cherenkov detection efficiency of $96 \pm 2(\text{stat}) \pm 0(\text{syst})\%$ with contamination of $6 \pm 3(\text{stat}) \pm 0(\text{syst})\%$.

After applying event selection criteria, 103 ring candidates were identified in the LAB/PPO data set. The topology of a typical event, and the average across the data set, are shown in Fig. 6. Again a clear ring structure can be observed. Hit-time residual distributions are

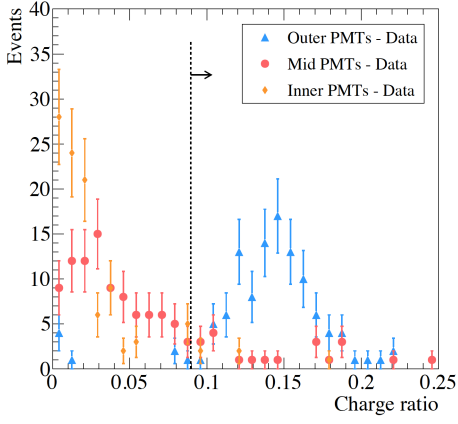


FIG. 5. Ratio of charge in a prompt, 5 ns window to the total charge for each hit PMT for pure LAB.

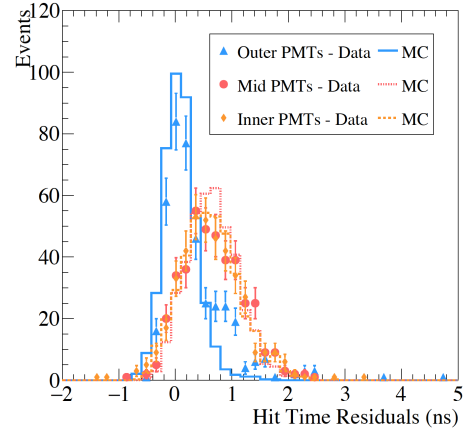


FIG. 7. Hit-time residual distributions in LAB/PPO for data and MC.

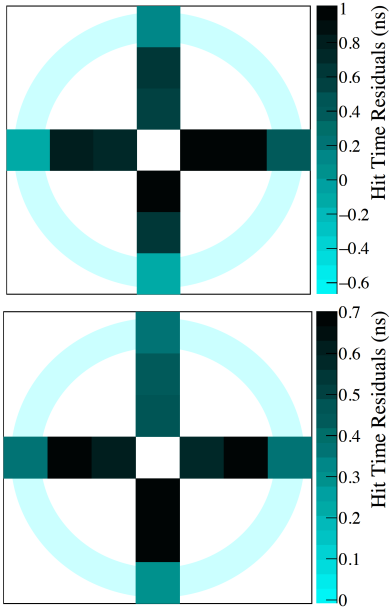


FIG. 6. Hit-time residuals versus PMT position for (Top) a single ring candidate event and (Bottom) the average across all events in LAB/PPO.

shown in Fig. 7, where the early Cherenkov hits on outer PMTs are clear. The separation is less distinct than for pure LAB, as expected. The MC shows good agreement with data. A cut at $t_c = 0.4$ ns yields Cherenkov detection efficiency of $70 \pm 3(\text{stat}) \pm 0(\text{syst})\%$ with contamination of $36 \pm 3(\text{stat}) \pm 4(\text{syst})\%$.

A scan of the LAB/PPO rise time, τ_r , showed that the data is inconsistent with zero rise time. The best χ^2 value for agreement between data and MC is for $\tau_r = 0.75$ ns. The data is consistent with $\tau_r = 0.5 - 1.0$ ns.

The charge ratio for LAB/PPO is shown in Fig. 8. The separation is more difficult in LAB/PPO due to higher scintillation yield. A threshold of $Q_{\text{ratio}} = 0.038$ gives a Cherenkov detection efficiency of $63 \pm 4(\text{stat}) \pm 7(\text{syst})\%$

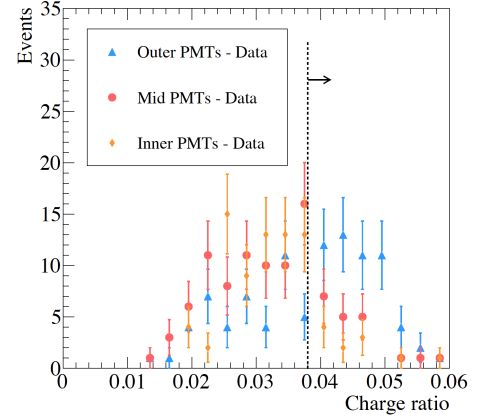


FIG. 8. Ratio of charge in a prompt, 5 ns window to the total charge for each hit PMT for LAB/PPO.

with contamination of $38 \pm 3(\text{stat}) \pm 2(\text{syst})\%$.

Successful time- and charge-based separation of Cherenkov and scintillation light has been achieved in both LAB and LAB/PPO with CHES. A time resolution of 338 ± 12 ps FWHM yields a Cherenkov detection efficiency in LAB/PPO of $70 \pm 3\%$ and $63 \pm 8\%$ for time- and charge-based separation, respectively, with scintillation contamination of $36 \pm 5\%$ and $38 \pm 4\%$. In pure LAB the time- and charge-based Cherenkov efficiencies are $83 \pm 3\%$ and $96 \pm 2\%$, with contaminations of $11 \pm 1\%$ and $6 \pm 3\%$. The LAB/PPO data is inconsistent with zero rise time, and consistent with a range of 0.75 ± 0.25 ns.

Demonstration of Cherenkov / scintillation separation at the PMT hit level opens new possibilities for optical detectors. Realizing this result in a large-scale scintillator detector such as SNO+ [16] would dramatically improve sensitivity to neutrinoless double beta decay by allowing rejection of the dominant ^8B solar neutrino background, as well as improving sensitivity to a range of physics topics including solar and supernova neutrinos.

This work was supported by the Laboratory Directed Research and Development Program of Lawrence Berkeley National Laboratory under U.S. Department of Energy Contract No. DEAC02-05CH11231. The work conducted at Brookhaven National Laboratory was supported by the U.S. Department of Energy under contract DE-AC02-98CH10886. The authors would like to thank the SNO+ collaboration for providing data on the optical properties of LAB/PPO, including the light yield, absorption and reemission spectra, and refractive index.

-
- [1] J. R. Alonso *et al.*, arXiv:1409.5864v3 [physics.ins-det] (2014).
 - [2] G. D. Orebi Gann for the THEIA interest group, in Proceedings of the Prospects in Neutrino Physics, arXiv:1504.08284 [physics.ins-det] (2015).
 - [3] M. Li *et al.*, arXiv:1511.09339 [physics.ins-det] (2015).
 - [4] J. Caravaca, F. B. Descamps, B. J. Land, J. Wallig, M. Yeh, and G. D. Orebi Gann, submitted to Phys. Rev. C (2016).
 - [5] https://www.hamamatsu.com/resources/pdf/etd/R11265U_H11934_TPMH1336E.pdf.
 - [6] <http://www.caen.it/csite/CaenProd.jsp?idmod=661&parent=11>.
 - [7] <http://www.eljentechnology.com/index.php/products/plastic-scintillators/ej-200-ej-204-ej-208-ej-212>.
 - [8] S. Seibert *et al.*, <http://rat.readthedocs.io/en/latest/>.
 - [9] M. Guan *et al.*, arXiv:1509.06176 [hep-ex] (2015).
 - [10] S. Agostinelli *et al.*, Nucl. Instrum. Methods Phys. Res. **A506**, 250 (2003).
 - [11] H. M. O’Keeffe, E. O’Sullivan, and M. C. Chen, Nucl. Instrum. Methods **A640**, 119 (2011).
 - [12] C. Buck & M. Yeh, J. Phys. G: Nucl. Part. Phys. **43** 093001 (2016).
 - [13] SNO+ Collaboration (private communications).
 - [14] B. von Krosigk, L. Neumann, R. Nolte, S. Röttger and K. Zuber, Eur. Phys. J. C **73**, 2390 (2013).
 - [15] I. Antcheva *et al.*, Comput. Phys. Commun. **180**, 2499-2512, (2009).
 - [16] S. Andringa *et al.* (SNO+ Collaboration), Adv. High Energy Phys. **2016**, 6194250 (2015).